Contrib Mineral Petrol (1983) 84:215–227

Contributions to Mineralogy and Petrology

The metamorphic evolution of garnet-cordierite-sillimanite-gneisses of the Gruf-Complex, Eastern Pennine Alps

Kurt Bucher-Nurminen[1] and Giles Droop[2]

[1] Mineralogical Institute, University of Basel, Bernoullistrasse 30, CH-4056 Basel, Switzerland
[2] Department of Geology and Mineralogy, University of Oxford, Parks Road, Oxford OX1 3PR, UK

Abstract. Metapelitic gneisses occuring as lenses and bands within the migmatites of the Gruf-Complex in the eastern Pennine Alps contain various combinations of the minerals quartz, biotite, cordierite, garnet, sillimanite, plagioclase, K-feldspar, spinel, orthopyroxene, anthophyllite and muscovite. The most common rock type is represented by a dark schistose biotite rich cordierite-garnet-sillimanite-gneiss. A consistent pressure-temperature range of 3–4 kb and 600–650° C has been calculated for the last metamorphic equilibration from six geological thermobarometers.

However, from textural evidence it may be concluded that the rocks were at both higher temperatures and pressures prior to the PT-conditions calculated from thermobarometry. Although the maximum conditions reached are unknown and earlier stages are poorly preserved it is suggested that they coincide with the maximum conditions deduced from rare occurrences of sapphirine granulite in the Gruf-Complex. These are 10 kb and 800° C (Droop and Bucher 1983). Sillimanite + K-feldspar, orthopyroxene + quartz, spinel + quartz and garnet-K-feldspar persisting in rocks with low activity of H_2O are strong evidence for this. The H_2O required to make the observed high degree of equilibration at 3–4 kb and 600–650° C possible was presumably released by crystallizing migmatitic melts present in the quartzo-feldspathic gneisses of the Gruf-Complex. Further evidence comes from the PT-coordinates of the H_2O-saturated muscovite granite solidus which coincides with the high temperature limits of inferred equilibration above and which the rocks must have crossed along the decompression and cooling path during their metamorphic evolution.

Introduction

Sapphirine-orthophyroxene granulites found at two localities within the migmatitic gneisses of the Gruf-Complex display evidence for a rather complex metamorphic history (Droop and Bucher 1983) and yield peak metamorphic conditions of 10 kb and 810° C. These conditions appear excessively high compared to the estimated regional metamorphic environment (Frey et al. 1974). The sapphirine-orthopyroxene granulites have been previously interpreted as relict tectonically emplaced fragments bearing the imprint of an older granulite facies metamorphism and showing little or no effect of the Alpine metamorphism (Frey et al. 1974).

Offprint requests to: K. Bucher-Nurminen

In this study we present textural and mineralogical data on cordierite-garnet-sillimanite gneisses occurring widespread in the Gruf migmatites. The deduced metamorphic history from phase petrology and geothermobarometry for these rocks supports an isofacial model for the sapphirine granulites within the Gruf complex, in contrast to earlier interpretations mentioned above.

The purposes of this contribution are:

1) To present new textural, mineralogical and mineral-chemical data on metapelitic rocks of the Gruf-complex which permit the calculation of the metamorphic conditions under which the rocks equilibrated and to elucidate the metamorphic history of the Gruf complex.

2) To compare these data with the metamorphic history deduced for the sapphirine granulites (Droop and Bucher 1983) and to discuss the geological implications on a regional scale.

Geological setting

The Gruf-complex represents a gneiss unit of complex structural and metamorphic history and of uncertain tectonic position in the Eastern Pennine Alps (Fig. 1). The migmatitic, isoclinaly folded Gruf gneisses can probably be correlated with the zone of Bellinzona-Dascio (Wenk 1973; Milnes and Pfiffner 1980, Wenk and Cornelius 1977; Trommsdorff 1980). The Gruf-complex is overlained by the Bergell intrusives along a sharp contact which is tectonic rather than intrusive. Structural elements in both units are parallel to the contact (Moticska 1970; Wenk 1973). The contact with the ophiolite zone of Chiavenna in the north of the Gruf-complex is characterized by a vertical strongly recristallized mylonite zone (Schmutz 1976). In the south the Novate granite clearly crosscuts both the Gruf gneisses and the Bergell intrusives. The relations to the Adula nappe to the west are unknown.

Very few studies are available on the internal structure and metamorphism of the Gruf complex. Schmutz (1976) described the northern contact zone between the Gruf mass and the Chiavenna ophiolites. Moticska (1970) studied the area southeast of Val Codera, and Wenk and Cornelius (1977) mapped the eastern part of the complex. Gulson (1973) concluded from his isotopic data on the Gruf migmatites that partial melting occurred during a pre-Alpine orogenic cycle. This interpretation was subsequently questioned by Wenk et al. (1974) who believed that the migmatites were formed during Alpine metamorphism.

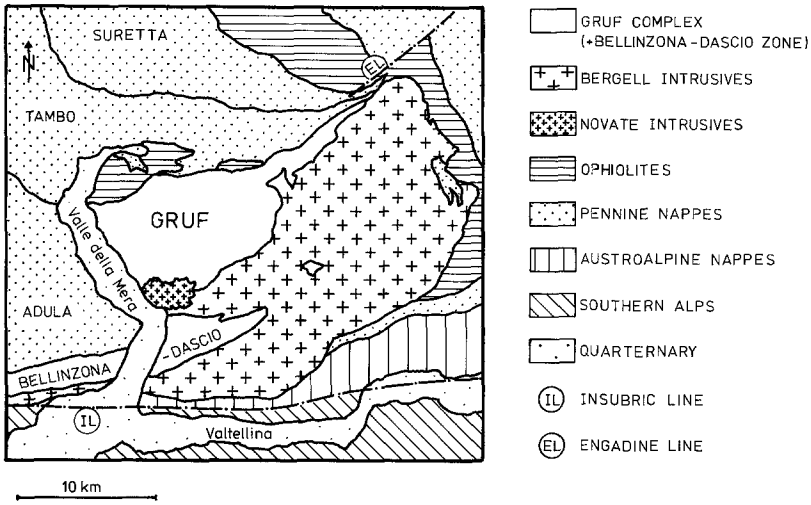

Fig. 1. Geological map of the Gruf area (after Trommsdorff 1980)

Metapelitic schists and gneisses occur as minor intercalations in a terrain composed predominantly of migmatitic quartzo-feldspathic gneisses. An uniform distribution pattern of mineral assemblages in metapelites has been reported by Wenk et al. (1974) suggesting similar metamorphic conditions across the Gruf-complex. Among the metapelitic gneisses cordierite-garnet-sillimanite-biotite gneisses represent the most common rock type. Alkalifeldspar + sillimanite has been reported from a number of localities, although widespread muscovite occurs as well. The two occurrences of sapphirine-orthopyroxene granulite have received attention by many geologists (Cornelius 1916; Cornelius and Dittler 1929; Barker 1964; Ackermand and Seifert 1968; Wenk et al. 1974), and have recently been studied in detail by Droop and Bucher (1983).

Other rock types of the Gruf-complex include ultramafic rocks, amphibolites and calcsilicate marbles (Moticska 1970). Very little information is available on these rare rock types (Wenk and Keller 1969 on amphibolites: Moticska 1970 on calcsilicate marbles).

Description of rock types

The mineral assemblages found in metapelitic rocks are listed in Table 1. The modal abundance of the minerals varies greatly, as does the appearance of the rocks in the field and hand specimen. The most common type however is represented by a dark, biotite-rich, gneissose rock (e.g. Al24, Al25, Al26 and Al36). Uniformly distributed small (typical grainsize ca. 2 mm) garnet grains are easily recognized, their modal abundance is typically less than 10 vol%. Sillimanite, biotite and cordierite can also be distinguished. Many of the samples are strongly foliated and banded. Dark biotite- and sillimanite-rich bands are separated by quartzo-feldspathic layers. These leucocratic layers also carry most of the cordierite. Very dark lenses consisting predominantly of biotite and minor sillimanite may also be present. The samples Al19, Al29 and Al40 are unusually rich in garnet (> 30%) and correspondingly poor in cordierite and biotite.

Discription of microtextures

The banded texture is also a prominent feature in thin section. Bands of granulose plagioclase, quartz and cordierite mosaic are separated by strongly schistose bands and lenses of biotite and sillimanite. Garnet may occur in both types of band.

Garnet. In most samples garnet is clearly a relict mineral (typical grainsize 1–2 mm). It shows very lobate and irregular outlines. Observed inclusion minerals are quartz, biotite, plagioclase, rutile, spinel and patches of sillimanite. The textures suggest that garnet is being replaced by biotite (Fig. 2a), biotite and sillimanite (Fig. 2b, 2c) and by cordierite. In sample Al19 and Al40 larger irregular garnets are replaced by clusters of recrystallized small subhedral grains. Texturally 'younger' garnets enclose sillimanite and spinel.

Sillimanite. Sillimanite occurs in four different textures; a) as fibrolite and small prismatic needles closely associated with biotite, in sillimanite-biotite bands or as shells around partially resorbed garnets (Fig. 2b). b) as monomineralic polycrystalline patches and streaks with no associated biotite (Fig. 2c). Sillimanite of this textural appearance may represent deformed pseudomorphs after kyanite. Kyanite has been reported from 2 samples from Gruf metapelites by Wenk et al. (1974) and Vogler (1983). c) together with cordierite replacing garnet, d) as inclusions in cordierite and garnet.

Cordierite. The textures suggest that cordierite is a relatively late mineral. It occurs predominantly in the plagioclase-quartz bands or together with sillimanite and/or biotite in aggregates replacing garnet. Garnet, spinel, sillimanite and biotite occur as inclusions in cordierite (Fig. 2d). In some rocks (e.g. Al26, Al27) cordierite is very abundant (> 30 vol%) and it is in mutual contact with all other minerals of the rock. Some textures (e.g. Al32) suggest that cordierite has grown together with biotite. In Al34 cordierite forms very large crystals (> 100 mm) and encloses anthophyllite.

Spinel. Green spinel was observed in 9 out of 16 examined samples as a modally subordinate mineral. Spinel occurs in three different textures: a) closely related and associated with sillimanite and garnet, b) as inclusions in cordierite (Fig. 2b) and garnet. c) In the assemblage sillimanite + plagioclase + biotite + spinel. In most samples spinel and

Table 1. Mineral assemblages of metapelitic gneisses

Sample	Locality	Coordinates	Qz	Sill	Bi	Gt	Cord	Plag	Sp	Other
Al19[a]	Bresciadega	761.2/125.3	×	×	×	×	×	×	×	rutil
Al23	Canino	761.8/128.4	×	×	×			×		Mu, Chl
Al24	Canino	761.8/128.4	×	×	×	×		×	×	Kfs, Mu
Al25[a]	Conco	761.8/128.1	×	×	×	×	×	×		
Al26[a]	Conco	761.8/128.1	×	×	×	×	×	×	×	
Al27	Conco	761.8/128.1	×	×	×	×	×	×		Mu, Kfs, Chl
Al28	Conco	761.8/128.1	×	×	×	×	×	×		Mu, Chl
Al29	Conco	761.8/128.1		×	×	×	×	×	×	Mu
Al29[a]	Conco	761.8/128.1		×	×	×	×	×	×	Mu
Al31	Conco	761.7/128.0	×	×	×		×	×	×	Opx, Ant
Al32	Vanninetti	763.9/129.4	×	×	×	×	×	×	×	Mu, Chl
Al33	Vanninetti	764.0/129.5	×	×	×			×		Mu
Al34	Vanninetti	763.8/129.3	×		×		×	×	×	Ant
Al35[a]	Vanninetti	763.9/129.4	×	×	×	×	×	×		
Al36	Vanninetti	763.9/129.4	×		×	×		×		Chl
Al37	Sivigia	763.7/129.3	×		×		×	×	×	Ant, Chl
Al40[a]	Conco	761.7/128.0	×	×	×	×	×	×	×	Mu
KV139	Vanninetti		×	×	×		×	×	×	Kfs, Mu, Chl
KV141	Vanninetti		×		×		×	×	×	Mu, Chl
KV148	Vanninetti		×	×	×	×	×	×		Kfs, Mu
KV153	Vanninetti		×	×	×	×		×		Kfs, Mu, Ky
KV163	Vanninetti		×	×	×		×	×		Mu, Chl
Sci278	Vanninetti	763.7/129.9	×	×	×			×		Mu, Chl
Sci623	Codera	762.0/128.5	×	×	×	×				Mu, Ky
Sci653	Averta	763.4/126.2	×	×	×			×		Mu, Chl
Sci400	Trubinasca	764.3/130.2	×	×	×		×			Kfs, Mu, Chl
Sci1018	Trubinasca	764.3/130.2	×	×	×		×			Kfs, Mu, Chl
Sci1019	Vanninetti	764.0/129.5	×	×	×		×	×		Mu, Chl
Cod6a[a]	Val Conco	761.7/128.0	×	×	×	×		×	×	Opx, Kfs
Cod23	Val Conco	761.7/128.0	×	×	×			×		Opx
Cod13a	Val Piana	760.6/127.3	×	×	×			×		Mu, Chl
Sci820	Val Piana	760.7/127.2	×	×	×		×	×	×	Opx, Kfs
Cod18c	Monte Gruf	759.3/126.5	×	×	×					Opx, Mu
Brg43b	Schiesone	752.7/129.2	×	×	×	×		×		
Mera48b	Schiesone	753.1/128.9	×	×	×		×			Mu
Mera36a	Trebecca	752.1/125.8	×	×	×	×		×		
Mot	Codera	?	×	×	×	×	×	×	×	Mu
HUS256	Gruf NR		×	×	×	×		×		Kfs, Mu
HUS700	Gruf NR		×		×	×		×		Kfs, Opx, Talc
HUS877	Gruf NR		×	×	×	×		×		Kfs

KV = Vogler (1983), Sci, Brg, Mera, Cod = Wenk et al. (1974), Mot = Moticska (1970), HUS = Schmutz (1976), Coordinates from Swiss coordinate net

[a] Sample analyzed on the electron microprobe

Abbrevations of mineral names:

Alm	Almandine	En	Enstatite	Oa	Orthoamphibole	Sill	Sillimanite
An	Anorthite	Gros	Grossular	Opx	Orthopyroxene	Sp	Spinel
Ant	Anthophyllite	Gt	Garnet	Phl	Phlogopite	Spes	Spessartine
Bi	Biotite	Kfs	K-feldspar	Plag	Plagioclase	Stau	Staurolite
Chl	Chlorite	Ky	Kyanite	Py	Pyrope	tsm	Tschermak component $Al_2Si_{-1}Mg_{-1}$
Cord	Cordierite	Mu	Muscovite	Qz	Quartz		

Sp = mineral or phase spinel; sp = component $MgAl_2O_4$

quartz are separated by a shell of cordierite of variable thickness. In sample Al32 spinel + quartz were found in direct grain contact. Spinel does not occur in contact with orthopyroxene or anthophyllite.

Biotite. Biotite is a major constituent in most samples and was found in contact with all other minerals.

Orthopyroxene. Coarse prismatic orthopyroxene shows preferred parallel orientation and was found in contact with anthophyllite, quartz, biotite, plagioclase and cordierite. Orthopyroxene has oriented inclusions of biotite and quartz and is partially replaced by anthophyllite.

Anthophyllite. Orthoamphibole occurs as patchy or blocky aggregates of up to 10 mm in diameter in the assemblage biotite + anthophyllite + cordierite + quartz. In sample Al31 epitactic overgrowth of anthophyllite on orthopyroxene was observed.

Muscovite and chlorite. Both minerals are clearly late alteration products related to shear zones or fractures or replacing cordierite and biotite in some samples.

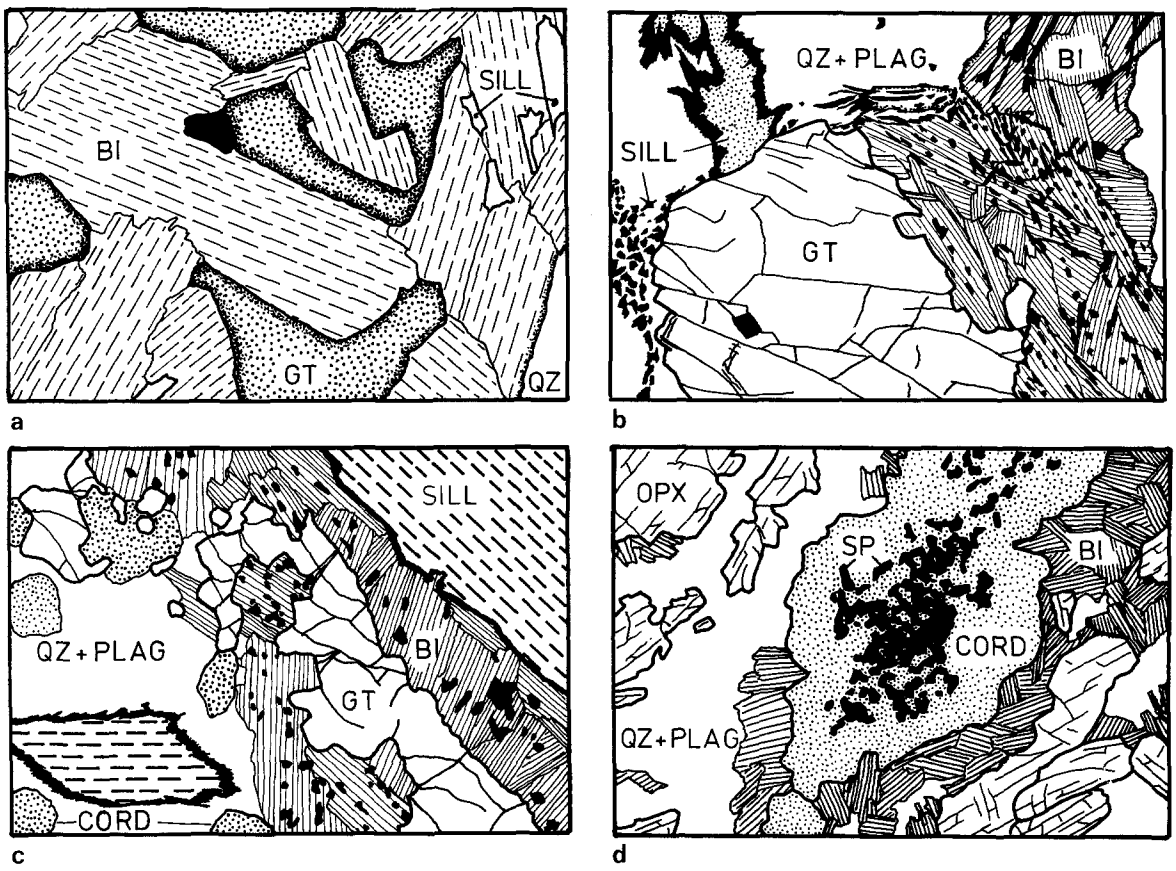

Fig. 2a–d. Typical textures from metapelitic rocks: (**a**) Biotite replacing garnet (Al36), (**b**) Partially resorbed garnet replaced by biotite + sillimanite (Al32), (**c**) biotite + sillimanite replacing garnet, monomineralic sillimanite bands and patches may represent deformed pseudomorphs after kyanite (Al26), (**d**) spinel mantled by cordierite, interpreted as product of the reaction Sp + Qz = Cord (Al31)

Mineral chemistry

The chemical composition of the minerals was obtained by using an energy dispersive electron microprobe at the Department of Geology of the University of Cambridge. Analyzed samples are marked with a superscript lower case a on Table 1[1]. The extent of $MgFe_{-1}$ and $(Mg, Fe)SiAl_{-1}$-Al_{-1} substitutions is shown on the histograms in Figs. 3, 4 and 5.

Garnets. The garnets show a weak zonation with pyrope-rich cores and almandine-rich rims. This general zoning pattern was detected consistently in all zoned garnets (Figs. 6 and 7). Because most of the garnets display characteristic resorption features and very irregular outlines, in detail rather different zoning profiles were obtained for different garnets of the same sample (e.g. Al25 garnets (Fig. 7). However, this shows that the zoning with respect to iron and magnesium may represent a growth feature and is probably not related to late resorption. The garnets show very little zonation with respect to grossular components. Garnet in the most common rock types represented by the analyses given on Fig. 7 show an enrichment in spessartine component towards the rims. This pattern of Mn-enrichment has been reported from resorbed garnets in other areas by Grant and Weiblen (1971) and deBethune et al. (1975), and

1 Microprobe analyses of garnet, biotite, cordierite, spinel, feldspar, orthopyroxene, and orthoamphibole of the samples marked with a superscript lower case a in Table 1 are available from the authors on request

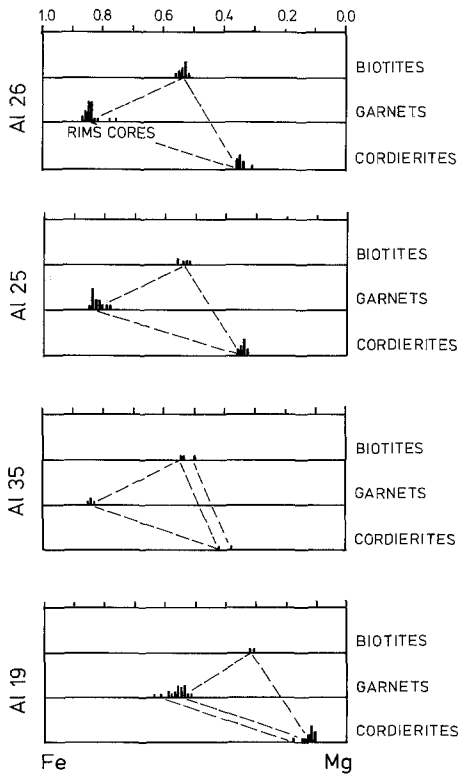

Fig. 3. Iron-magnesium variation histograms for biotite, garnet and cordierite. Smallest dash represents one analysis

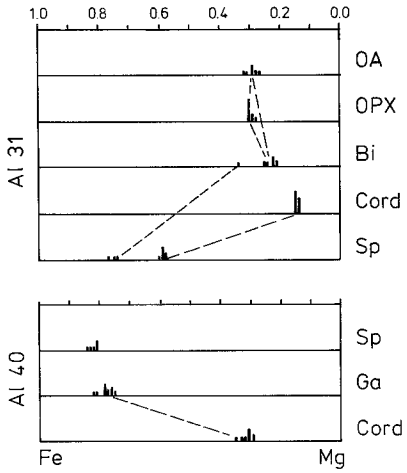

Fig. 4. Iron-magnesium variation histograms for minerals of the samples Al31 and Al40. Smallest dash represents one analysis

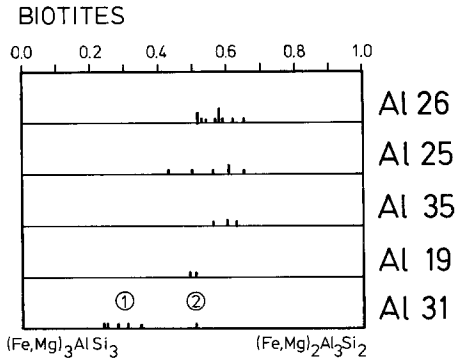

Fig. 5. Tschermak substitution histograms for biotite. 1) and 2) represent compositions from chemically different domains of the sample

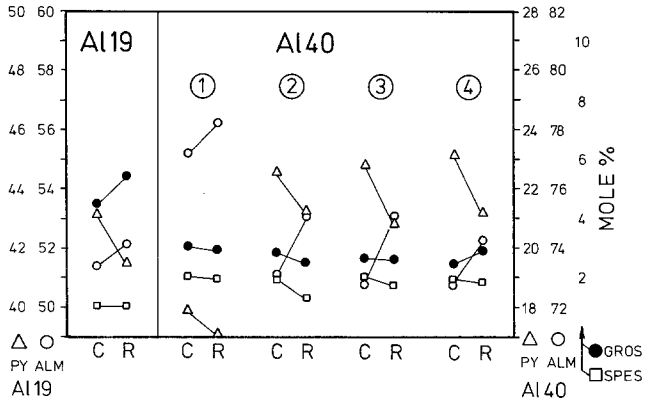

Fig. 6. Chemical zonation of garnet in samples Al19 and Al40 (C, core; R, rim; numbers in circles: different grains of the same sample)

seems to be a very characteristic resorption feature. Fe/Fe+Mg ratios vary within narrow limits between 0.75 and 0.85 for the common garnet-biotite-cordierite-sillimanite gneisses, but may be as low as 0.55 in Al19.

Biotite. Fe/Fe+Mg ratios of 0.50–0.55 were found in most samples analyzed and the extent of tschermak substitution centers around 50 to 60 mol %. It was found however, that biotite of the sample Al31 in the assemblage biotite+spinel had a similar amount of tschermak substitution (No. 2, Fig. 5) but biotite in the assemblage biotite+cordierite+orthopyroxene is significantly closer to pure phlogopite-annite solutions (No. 1, Fig. 5).

Cordierite. Cordierites are very homogeneous chemically. Fe/Fe+Mg ratios are near 0.35 for garnet-cordierite-biotite-sillimanite gneisses. In the magnesian metapelites (Al19 and Al31) Fe/Fe+Mg ratios of 0.1–0.15 were measured.

Spinel. All spinels analyzed are essentially hercynite-spinel solutions. Gahnite, magnetite and other endmember spinel components total less than 10 mol %. The composition of spinel of Al31 shows a clear correlation with the local mineral assemblage. Spinel coexisting with biotite+sillimanite+plagioclase was found to be significantly enriched in gahnite and hercynite component compared to spinel coexisting with cordierite.

Orthopyroxene. The chemical variation found within orthopyroxene may be described by the $MgFe_{-1}$ and (Mg, Fe) $SiAl_{-1}Al_{-1}$ substitutions on enstatite. The measured concentrations of Al_2O_3 varies between 2.4 and 4.6 wt.%. Orthopyroxene does not coexist with garnet in most of our samples. The orthopyroxenes are zoned with respect to both substitutions above (Fig. 8). Cores of prismatic orthopyroxene are enstatite-rich, but ferrosilite and tschermak components increase towards the rims.

Orthoamphibole. The analyzed orthoamphibole are very low in alkalies and calcium in contrast to orthoamphiboles from similar rocks analyzed by Grant (1981). Two substitutions account for the chemical variation found in the Gruf amphiboles modifying the anthophyllite endmember composition. These are the $MgFe_{-1}$ and the (Mg, Fe)$SiAl_{-1}Al_{-1}$ substitutions. Endmember calculations using the procedure given by Misch and Rice (1975) indicate that the orthoamphiboles may be regarded as binary anthophyllite (81–92) – tschermakite (18–7) solutions[2].

Plagioclase. Plagioclase show a fairly uniform composition in each sample. The anorthite content of plagioclases from different samples varies between An(25) and An(90).

Alkalifeldspar. The compositional range of K-feldspar (microperthite) of Ab(13) Or(87) to Ab(15) Or(85) is similar to analyzed K-feldspars in the sapphirine granulites (Droop and Bucher 1983).

Geothermometry and geobarometry

The widespread minderal assemblage cordierite-biotite-garnet-plagioclase-quartz-sillimanite enables estimates to be made of the pressure and temperature conditions under which the rocks equilibrated. The experimental or empirical calibrations of the equilibria listed below were used for the *PT*-calculations (exchange component notation adopted from Thompson (1982).

$$MgFe_{-1}(\text{biotite}) = MgFe_{-1}(\text{garnet}) \quad (1)$$

Holdaway and Lee (1977), Ferry and Spear (1978). Thompson (1976)

$$MgFe_{-1}(\text{cordierite}) = MgFe_{-1}(\text{garnet}) \quad (2)$$

Thompson (1976), Holdaway and Lee (1977)

2 Due to the high detection levels of sodium on the EDS microprobe it cannot be excluded that some edenite substitution occurs in addition to the observed tschermak substitution

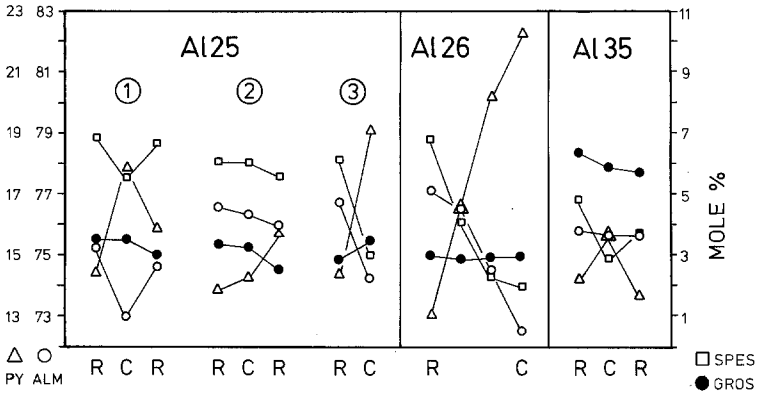

Fig. 7. Chemical zonation of garnet in samples Al25, Al26, and Al35 (C, core; R, rim; numbers in circles: different grains of the same sample)

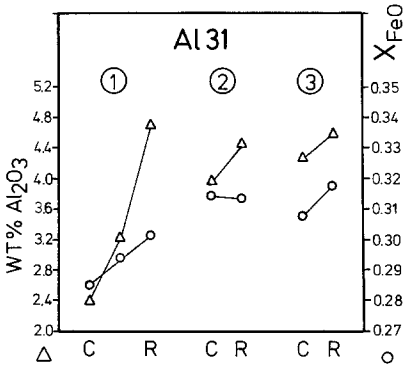

Fig. 8. Chemical zonation of orthopyroxene in sample Al31 (C, core; R, rim; numbers in circles: different grains)

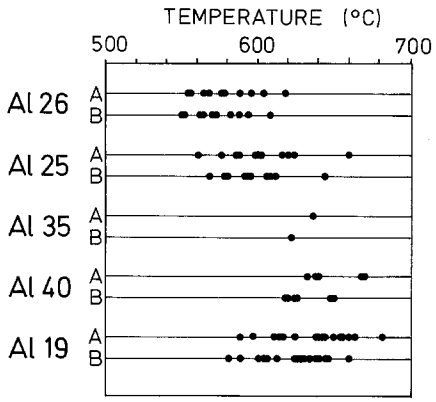

Fig. 9. Calculated temperatures from the garnet-cordierite Fe–Mg exchange thermometer at 5 kb. A, Thompson (1976); B, Holdaway and Lee (1977). Each dot represents the temperature calculated from one pair in mutual grain contact

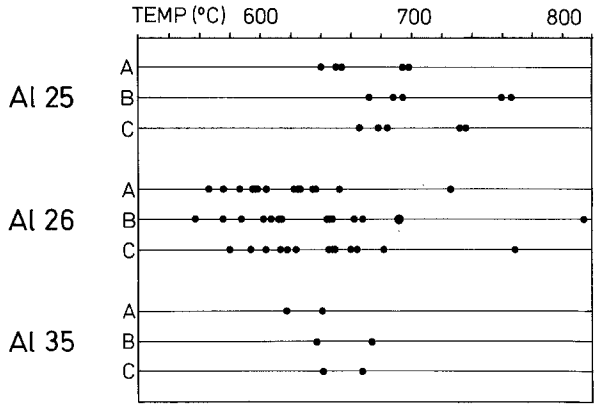

Fig. 10. Calculated temperature from the garnet-biotite Fe–Mg exchange thermometer at 5 kb. A, Holdaway and Lee (1977); B, Ferry and Spear (1978); C, Thompson (1976). Each dot represents the temperature calculated from one pair in mutual grain contact

$$3\ CaAl_2Si_2O_8 = Ca_3Al_2Si_3O_{12} + 2\ Al_2SiO_5 + 1\ SiO_2 \quad (3)$$
an (in plag) gros (in gt) sill qz

Schmid and Wood (1976), Ghent et al. (1979), Newton and Haselton (1981), Aranovich and Podelesskiy (1980)

$$3\ Fe_2Al_4Si_5O_{18} = 2\ Fe_3Al_2Si_3O_{12} + 4\ Al_2SiO_5 + 5\ SiO_2 \quad (4)$$
Fe-cord (in cord) alm (in gt) sill qz

Thompson (1976), Holdaway and Lee (1977), Wells and Richardson (1980), Newton and Wood (1979).

The coexistence of K-feldspar and plagioclase as well as orthopyroxene and garnet in the leucocratic portion of the sample Cod6a permits *PT*-estimates from two additional equilibria:

$$NaK_{-1}\ (\text{K-feldspar}) = NaK_{-1}(\text{plagioclase}) \quad (5)$$

Stormer and Whitney (1977)

$$(Mg,Fe)_3Al_2Si_3O_{12} = (Mg,Fe)_3Al_2Si_3O_{12} \quad (6)$$
(orthopyroxene) (garnet)

Wood (1974), Harley and Green (1982)

Temperatures calculated from equilibrium 1 are shown on Fig. 9 and from equilibrium 2 on Fig. 10. Excluding the garnet-biotite pairs of Al25 and Al26 which resulted in very high temperatures, the scatter of calculated temperatures is on the order of 100–120 deg.C around a mean temperature of about 620 deg.C for Al26, 670 deg.C for Al25 and 640 deg.C for Al35. The scatter for garnet-cordierite temperatures is somewhat smaller and the mean temperature for Fe-rich metapelites (Al25 and Al26) is close to 580 deg.C. Temperatures calculated for garnet-cordierite pairs from magnesian metapelites (Al19 and Al40) are slightly higher, between 620 and 630 deg.C. The temperatures calculated from the different literature sources agree reasonably well with one another for both thermometers. The temperatures given on Figs. 9 and 10 respectively are shown as dashed variation bands on the *PT*-diagrams of Fig. 12 (the very high temperature garnet-biotite pairs of Al25 and Al26 excluded).

Pressures calculated from equilibrium 3 are represented on Fig. 11. The results from the different calibrations overlap reasonably for the Fe-rich metapelites.However, garnet-

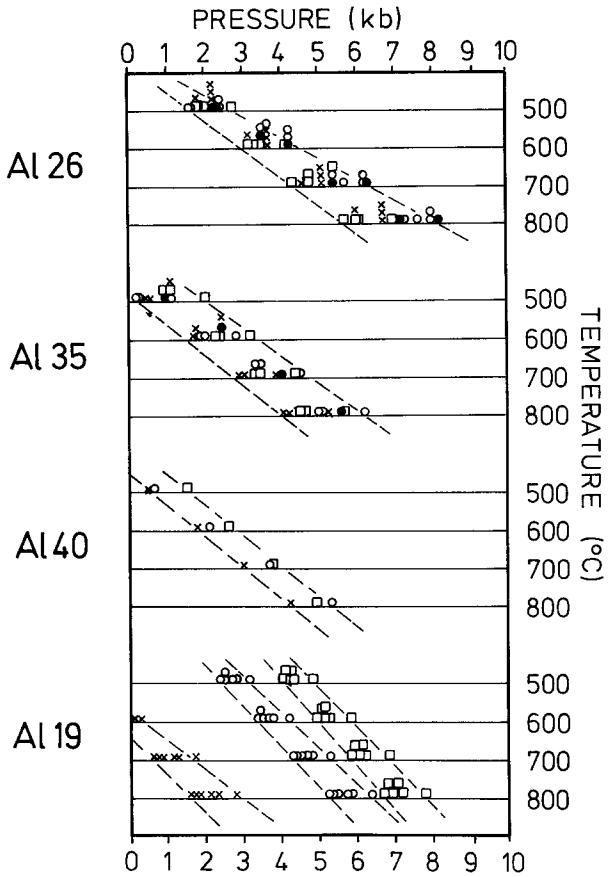

Fig. 11. Calculated pressures from the assemblage Gt+Plag+Sill+Qz at 4 different temperatures. Circles, Schmid and Wood (1976); squares, Aranovich and Podelesskiy (1980); Crosses, Ghent et al. (1979); filled circles, Newton and Haselton (1981). Each symbol represents pressures calculated from one garnet-plagioclase pair in mutual contact near sillimanite and quartz

plagioclase pressures calculated for Al19 (Mg-rich metapelite) show a marked separation for the different calibrations. For this sample we ignored the results from the calibration given by Ghent et al. (1979). The pressures given on Fig. 11 are again shown as dashed variation bands on Fig. 12.

In contrast to equilibrium 3 (plagioclase + garnet + sillimanite + quartz) which is strongly temperature dependent, the assemblage cordierite + garnet + sillimanite + quartz represents an excellent barometer with a very small slope for the equilibrium conditions of reaction 4 in *PT*-space. The calculations using the calibrations from the sources above, however, resulted in pressures generally about one to two kilobars too high to give a *PT*-field in common to all four thermobarometers used. We therefore calculated pressures from equilibrium 4 formulated for the Mg-endmembers rather than Fe-endmembers using recently derived internally consistent thermodynamic data for cordierite and pyrope (Bucher et al. in prep). The data and calculation procedure are given in the appendix. The pressure variation bands on Fig. 12 are based on our own calibration of equilibrium 4 assuming H_2O-saturated cordierite for Al25, Al26 and Al35. For Al19 the pressure band shown represents the full range between H_2O-saturated and dry cordierite. The pressures calculated for Al19 overlap with the pressures from the other samples only if cordierite of Al19 had a low H_2O-content. The equilibrium 4 is also shown on Fig. 14 for different H_2O-content in cordierite. A more detailed discussion of Fig. 14 will follow in the next section.

Coexisting K-feldspar and plagioclase in sample Cod6a revealed solvus temperatures of 610° C at 5 kb and 668° C at 10 kb using the microcline calibration of Stormer and Whitney (1977), sanidine temperatures are about 50° C lower.

Orthopyroxene – garnet pressures for the same sample (leucocratic portion) range between 2.5–3.5 kb at 700° C and 6.5–7.5 kb at 800° C using the calibration of Wood (1974). Slightly lower pressures for a given temperature were calculated from the recent calibration of Harley and Green (1982).

The results of the thermobarometry are summarized on Fig. 12 for some of the samples separately. The data permit the selection of a reasonably well defined *PT*-range for the last supposed chemical equilibration at 3 to 4 kb and 600 to 650° C. This pressure temperature range has been plotted together with the deduced *PT*-path for the Gruf sapphirine granulites on Fig. 16 (Droop and Bucher 1983). From this Fig. 16 it may be concluded that the Fe-rich metapelites reequilibrated along the retrograde portion of the regional *PT*-path and lost their memory with respect to earlier stages whereas the magnesian metapelites did not (provided that these different rock types indeed had the same *PT*-path in common. Evidence for this will be given later). The reason for the apparently different memory may be related to the fact that above the staurolite 'out' isograd in Fe-rich metapelites the assemblage biotite + alumosilicate + garnet + K-feldspar persists up to granulite facies conditions. In Mg-rich metapelites a variety of additional phases may appear in the assemblages such as spinel, orthopyroxene, orthoamphibole, sapphirine, osumilite and kornerupine. These minerals and their various assemblages may record the high grade metamorphic history more sensitively than the Gt + Als + Bi + Kfs assemblage in Fe-rich metapelites. In the latter rocks garnet zoning patterns may be the only key to assess the high grade history of the rock. In addition under high grade conditions the garnet zoning patterns may gradually become extinguished as a result of volume diffusion and homogenization (Woodsworth 1977; Yardley 1977). However, garnets from the Gruf sapphirine granulites which may have been at temperatures in excess of 800° C (Droop and Bucher 1983) and the garnets analyzed for this study still display a distinct growth zonation.

Temperature and pressure estimates available in the literature for rocks of the Gruf-complex refer exclusively to the sapphirine granulite from the Bresciadega locality and have been discussed by Droop and Bucher (1983).

Interpretation of textures and mineral reactions

The observed garnet resorbtion and its replacement by sillimanite and biotite can be explained as the result of the reaction:

$$1\ Gt + 1\ Kfs + 1\ H_2O \rightarrow 1\ Sill + 1\ Bi + 2\ Qz \quad (7)$$

Under equilibrium conditions the following equilibria must hold simultaneously

$$1\ py + 1\ kfs + 1\ H_2O = 1\ sill + 1\ phl + 2\ qz \quad (8)$$

$$3\ tsm(bi) = 2\ qz + 1\ py - 2\ sill \quad (9)$$

$$FeMg_{-1}(Bi) = FeMg_{-1}(Gt) \quad (10)$$

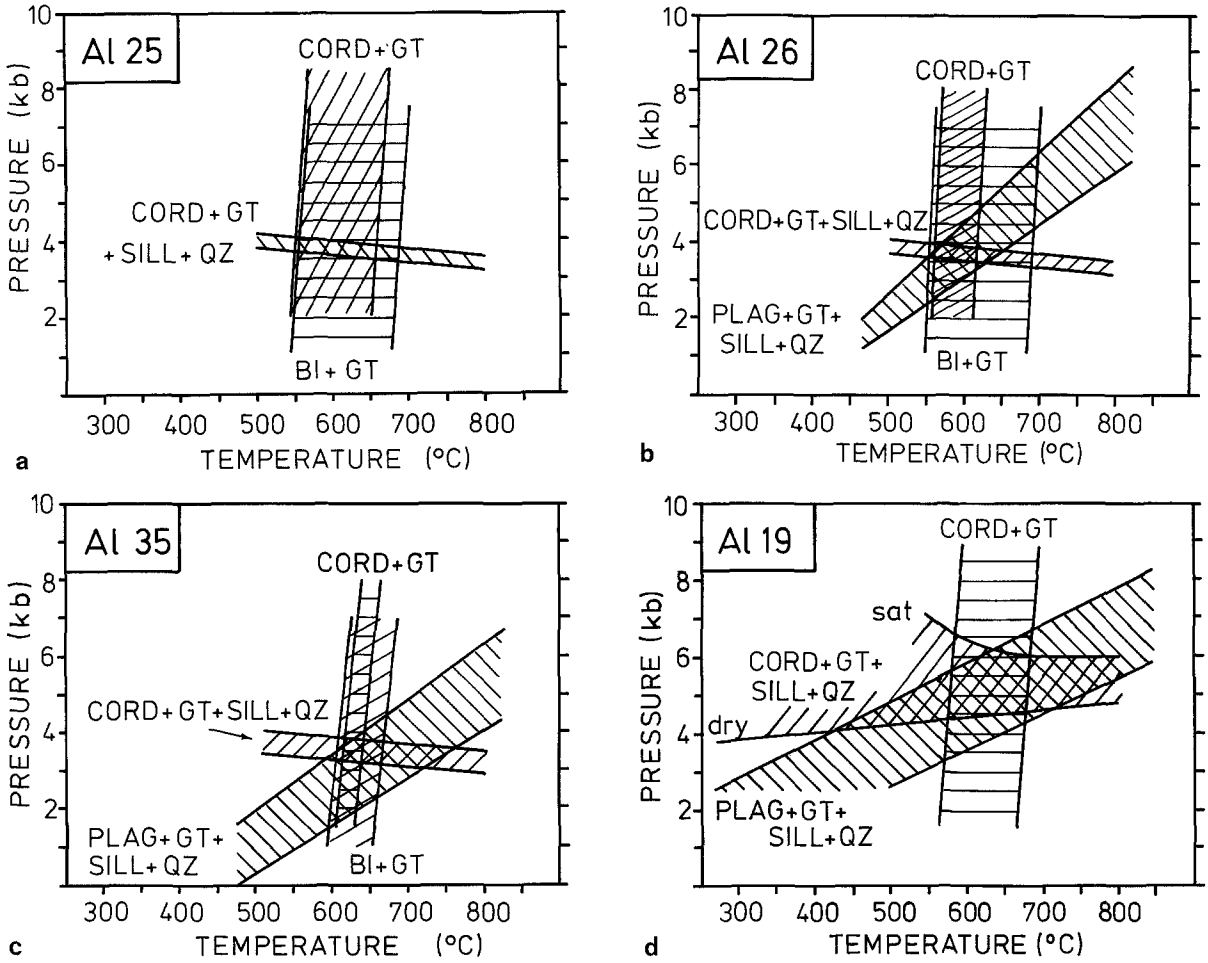

Fig. 12a–d. Summary of thermobarometric data for four different samples. For Al19 Gt+Plag pressures calculated from Schmid and Wood (1976) and Aranovich and Podelesskiy (1980) only

Buehl (1980) gave qualitative *PT*-coordinates for the assemblage Gt+Kfs+Sill+Bi+Qz and predicted that the tsm-component in biotite should decrease with decreasing *P* and *T* (positive slope of equilibrium conditions). Figure 13 shows the *PT*-coordinates for equilibrium 8 for two different samples (for activity-composition relations and calculation procedures for all equilibria discussed in this section see appendix). The two curves refer to the condition of $a_{(H_2O)}=1.0$. It can be seen in Fig. 13 that the two curves for the retrograde sillimanite+biotite formation according to reaction 7 envelop the *PT*-box from the independent thermobarometry. It also may be concluded that the rocks may have been at higher pressures and temperatures prior to equilibration under the conditions of the '*PT*-box'. Furthermore, the H_2O-pressure was apparently near the load pressure at least for the Fe-rich metapelites.

Garnet is also being consumed according to the reaction:

$$2\,\text{Gt}+4\,\text{Sill}+5\,\text{Qz}\rightarrow 3\,\text{Cord} \qquad (11)$$

The equilibrium conditions of this cordierite producing reaction is nearly independent of *T* and has been used in the previous section for pressure estimates. The textures suggest that cordierite formed at the expense of garnet indicating cordierite formation along a decompression path (Fig. 14). Euhedral garnets with no resorption features

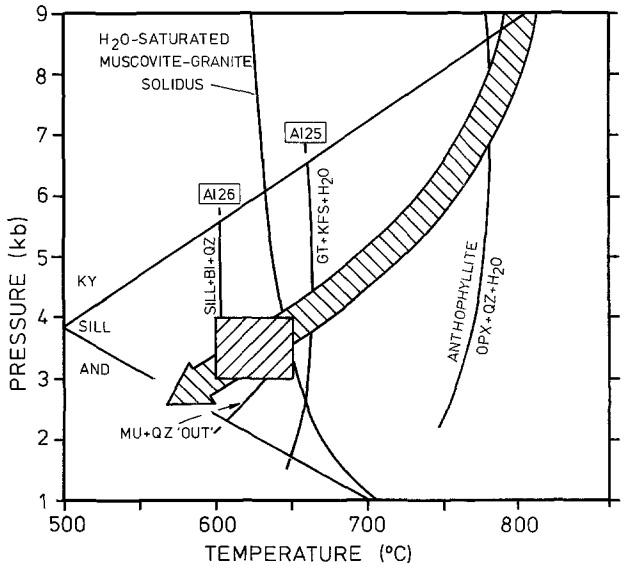

Fig. 13. Dashed box, *PT*-conditions from thermobarometry; dashed arrow, cooling and uplift path deduced from Gruf sapphirine granulites (Droop and Bucher 1983). Granite solidus after Wyllie (1977), equilibrium conditions of the garnet resorbing reaction 7) for mineral compositions of Al25 and Al26 respectiveley, lower temperature limit of Opx+Qz (reaction 22) for mineral compositions of Al31 and the reaction 24) (all equilibria for $a_{H_2O}=1$). Source of data given in the appendix

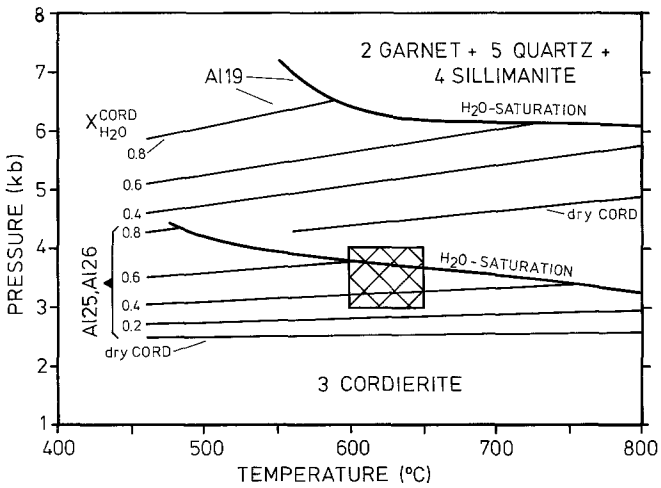

Fig. 14. Equilibrium conditions of the reaction 11: $6 \log K_D = 1.7$ (Al19) and 3.5 (Al25, Al26). Contours are for different H_2O-contents of cordierite. Crosshatched area: suggested PT-conditions from thermobarometry (data given in the Appendix)

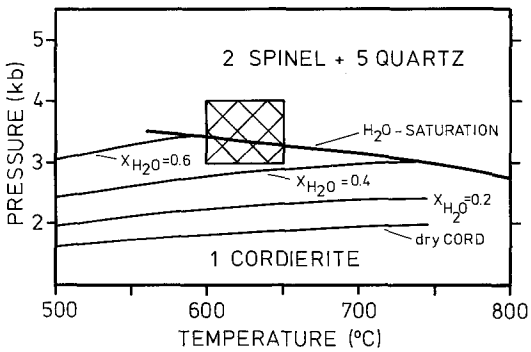

Fig. 15. Equilibrium conditions of the reaction 14 calculated from the data given in the appendix. Crosshatched box: suggested PT-conditions from thermobarometry. The diagram is contoured for 4 different mol fractions of H_2O in cordierite. $2 \log K_D = 0.633$ (Al31)

overgrew spinel and sillimanite a texture which may have resulted from the reaction:

$$5\ Qz + 3\ Sp \rightarrow 2\ Sill + 1\ Gt \quad (12)$$

However, this texture is of minor importance and has been included here for completeness. If the interpretation of monomineralic sillimanite patches and streaks as pseudomorphs after kyanite is correct, then the rocks also underwent the reaction:

$$1\ Ky \rightarrow 1\ Sill \quad (13)$$

It should be remembered that rare kyanite relicts have been reported by Wenk et al. (1974) and Vogler (1983) from Gruf metapelites.

The textural relations involving cordierite suggest that it does not represent a cogenetic prograde mineral with garnet, but rather indicate cordierite production relatively late in the metamorphic history of the rocks. It may coincide with the sillimanite + biotite formation from garnet according to reaction 7. As concluded from reaction 11 cordierite formation may have resulted from decompression. This conclusion is further supported by spinel + cordierite textures (Fig. 2d) which are probably the consequence of the reaction:

$$5\ Qz + 2\ Sp \rightarrow 1\ Cord \quad (14)$$

In Fig. 15 the equilibrium conditions for reaction 14 are given for the chemical composition of minerals of sample Al31 using activity-composition relations listed in the appendix. Cordierite formation again requires decompression and the rocks were at higher pressures prior to equilibration at *PT*-conditions calculated from thermobarometry. Furthermore, the only curve that passes reasonably through the thermobarometric '*PT*-box' in Fig. 15 is the one calculated for H_2O-saturated cordierite. This again suggests high H_2O-activity at the retrograde equilibration stage.

At the stage of cordierite formation the assemblage spinel + cordierite was apparently more stable than garnet + sillimanite. The two alternative assemblages are related by the equilibrium:

$$1\ sp + 1\ cord = 2\ sill + 1\ py \quad (15)$$

Simultaneous growth of biotite and cordierite observed in some samples (e.g. Al32) may be explained by hydration reactions of the type:

$$6\ Gt + 4\ Kfs + 4\ H_2O \rightarrow 3\ Qz + 3\ Cord + 4\ Bi \quad (16)$$

(in Qz-saturated rocks or domains in rocks) and

$$9\ Gt + 5\ Kfs + 3\ Sill + 5\ H_2O \rightarrow 6\ Cord + 5\ Bi \quad (17)$$

(in Qz-deficient rocks or domains of rocks)
The observed reaction relation in sample Al34 where cordierite replaces anthophyllite may be written as

$$48\ Sp + 15\ Ant + 20\ H_2O + 35\ Kfs \rightarrow 24\ Cord + 35\ Bi \quad (18)$$

In this sample abundant spinel and anthophyllite are not in mutual grain contact.

Spinel inclusions in cordierite have been interpreted as the educt minerals of reaction 14. However, spinel inclusions in garnet which frequently occur together with sillimanite probably represent a prograde feature and may be related to the breakdown of staurolite once present by the reaction (in Qz-deficient rocks):

$$10\ Stau \rightarrow 3\ Gt + 11\ Sp + 31\ Sill\ (Ky?) + 5\ H_2O \quad (19)$$

It is interesting to note in this context that spinels coexisting with sillimanite in sample Al31 contain three times as much gahnite component as spinel from the same sample but coexisting with cordierite (Table 5). At some stage during the metamorphic evolution spinel occurred not only in Qz-deficient areas together with sillimanite but must have coexisted with quartz as well (evidence comes from reaction 14). Thus the assemblage spinel + quartz was probably common at an early stage of the metamorphic evolution. In sample Al31 relictic (metastable?) quartz + spinel is still present. This two phase assemblage was then replaced by cordierite by reaction 14. In very magnesian metapelites quartz + spinel was converted into sapphirine prior to the cordierite formation (Droop and Bucher 1983). The supposed quartz + spinel assemblage may have formed from a prograde reaction:

$$1\ Bi + 3\ Sill(Ky) \rightarrow 3\ Sp + 1\ Kfs + 3\ Qz + 1\ H_2O \quad (20)$$

Oriented inclusions of biotite and quartz in orthopyroxene are evidence for the reaction:

$$3\ Qz + 1\ Bi \rightarrow 3\ En + 1\ Kfs + 1\ H_2O \quad (21)$$

Reaction 21 may have been responsible for the formation

of orthopyroxene. In contrast to the mineral assemblages of the Fe-rich metapelites, the assemblage of equation 21 requires low H_2O activities at 4 kb and 600 to 650° C. Calculated H_2O activities at 4 kb and the temperatures above are 0.03 and 0.04 respectively. Epitactic overgrowth of anthophyllite may be explained by the reaction:

$$7\ \text{En(Opx)} + 1\ \text{Qz} + 1\ H_2O \rightarrow 1\ \text{Ant} \qquad (22)$$

The observed assemblage Opx + Qz + Ant in Al31, Al19 and Al40 magnesian metapelites buffer the activity of H_2O at 4 kb to low values (0.21 at 600° C and 0.325 at 650° C). The PT-coordinates for equilibrium 22 for $a_{H_2O} = 1.0$ and mineral compositions of sample Al31 are shown on Fig. 13. Prograde formation of anthophyllite in sample Al34 could have resulted from reaction:

$$24\ \text{Qz} + 7\ \text{Bi} \rightarrow 3\ \text{Ant} + 7\ \text{Kfs} + 4\ H_2O \qquad (23)$$

by analogy to reaction 21.

The metamorphic conditions deduced from the geothermobarometry are consistent with the stable coexistence of muscovite + quartz. Texturally however, muscovite is clearly a late retrograde mineral, and has probably formed from the reaction:

$$1\ \text{Kfs} + 1\ \text{Sill} + 1\ H_2O \rightarrow 1\ \text{Mu} + 1\ \text{Qz} \qquad (24)$$

The equilibrium conditions for reaction 24) are shown on Fig. 13 labelled as "Mu + Qz 'out'" curve for unit water activity. From the position of this curve with respect to the '*PT*-box' and the observed relict assemblage sillimanite + K-feldspar it may be concluded that reequilibration of the rocks occurred under high H_2O-activity and that the rocks were once at higher metamorphic grade. The calculated H_2O activities at 4 kb and 600° C and 650° C are 0.53 and 0.90 respectively. Two other equilibria permit the calculation of H_2O activities at the inferred pressure temperature conditions of equilibration; these are:

$$6\ \text{Sill} + 9\ \text{Qz} + 2\ \text{Bi} = 3\ \text{Cord} + 2\ \text{Kfs} + 2\ H_2O \text{ and} \qquad (25)$$

$$6\ \text{Mu} + 15\ \text{Qz} + 2\ \text{Bi} = 3\ \text{Cord} + 8\ \text{Kfs} + 8\ H_2O \qquad (26)$$

Using the mineral composition of sample Al26 and the activity composition relations given in the appendix the following H_2O activities resulted from the calculation at 4 kb: For equilibrium 25) 0.5 at 600° C and 0.76 at 650° C, for equilibrium 26) 0.53 at 600° C and 0.86 at 650° C.

One problem must be addressed at this point. The pressure temperature conditions calculated from thermobarometry are just below the conditions of the H_2O-saturated muscovite-granite solidus (Wyllie 1977). The PT-coordinates for the H_2O-saturated muscovite-granite solidus are also shown on Fig. 13. If, as suggested, the rocks have been at higher pressures and temperatures at some earlier stages during metamorphic evolution this would imply conditions inside the *PT*-field for granitic melt formation. Partial melting is in fact indicated by the widespread migmatitic textures in quartzo-feldspathic gneisses of the Gruf-complex and by K-feldspar patches and veinlets in many of the metapelitic gneisses. The stable coexistence of orthopyroxene + quartz and K-feldspar + sillimanite under H_2O-rich conditions also requires temperatures clearly within the melting field of 'wet' granite. The reactions involving K-feldspar formulated on the previous pages may thus involve a melt phase rather than solid K-feldspar. This melt phase probably stored a large amount of the H_2O given off by the prograde mineral reactions such as dehydration of muscovite, biotite and probably staurolite. Along the cooling and uplift path this H_2O was released by the solidifying melt again. It was partially fixed in the micas of the leucocratic portion of the migmatites. Excess H_2O expelled from the migmatites on crystallisation could account for the high degree of reequilibration under conditions of high H_2O-activity observed at pressures and temperatures just below the granite solidus. Very magnesian metapelites apparently were less accessible to late H_2O and therefore preserved earlier stages of the metamorphic history. An extreme case of this behaviour are the sapphirine rocks of the Gruf area.

Summary and geological interpretation

The metapelitic rocks of the Gruf-complex may be divided into two groups on the basis of mineralogical composition, mineral and bulk chemistry.

1) Iron-rich metapelites typically contain cordierite + garnet + biotite + sillimanite + plagioclase + quartz ± spinel. Cordierite in these samples contains about 60–70 mol % Mg-cordierite component. Thermobarometry on these rocks defines a relatively narrow and consistent *PT*-range of presumed equilibration at 3–4 kb and 600–650° C, under conditions of high water activity. These conclusions compare favourably with calculated dehydration equilibria relevant to the rocks. However, the *PT*-conditions of equilibration given above very likely do not represent the maximum conditions reached by the rocks during their metamorphic evolution. This conclusion was derived from compositional zoning found in garnets and orthopyroxenes (the latter in magnesian metapelites, see below) and from textural observations. Many of the observed textures imply that dehydration reactions run from the high temperature to the low temperature side and consequently are rehydration reactions. The H_2O required to make this equilibration possible was presumably released by cristallizing migmatitic melts, a conclusion derived from the widespread occurrence of migmatites in the Gruf-complex and from the *PT*-coordinates of the H_2O-saturated muscovite granite solidus which coincides with the high temperature limits of inferred equilibration given above.

2) Magnesium-rich metapelites show a wider variety in mineralogical composition compared to the rocks above. Additional minerals observed are orthopyroxene, orthoamphibole and sapphirine. The petrology of sapphirine-bearing metapelites has been discussed elsewhere (Droop and Bucher 1983). Spinel is abundant in these rocks whereas garnet may not be present. Here, cordierite typically contains 90 mol % Mg-cordierite. Thermobarometry on these rocks suggests the same *PT*-range for equilibration conditions. However, garnet-cordierite-sillimanite-quartz pressures of about 4 kb are indicated only if dry cordierite is assumed to be present. Low activities of H_2O are also suggested by H_2O-involving equilibria relevant to the magnesian metapelites. Calculated H_2O-activities for these rocks are typically below 0.2. There is no conclusive explanation for the different H_2O-activities during equilibration of the two rock typs, but the dense magnesian metapelites were apparently less accessable to H_2O released by crystallizing migmatitic melts. The rocks are less schistose and generally contain less modal biotite.

The textures and the mineral reactions deduced from them suggest that the rocks were at both higher tempera-

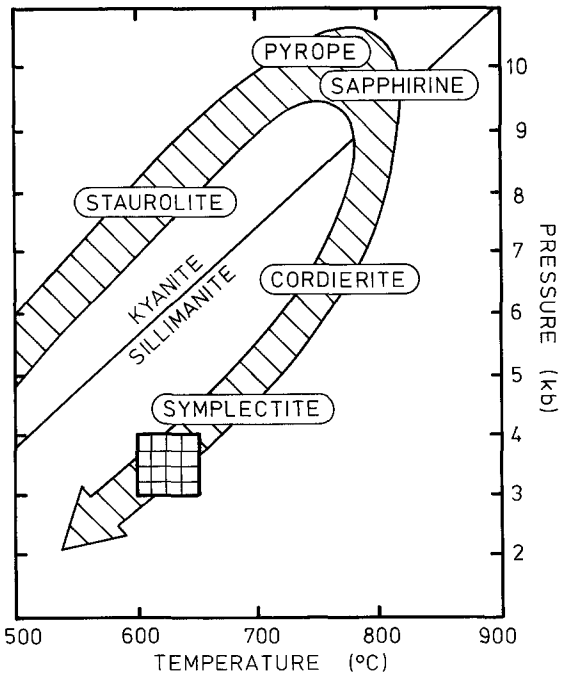

Fig. 16. *PT*-conditions of Gruf metapelites (crosshatched box) compared to the path of metamorphic evolution of Gruf sapphirine granulites (arrowed loop, from Droop and Bucher 1983)

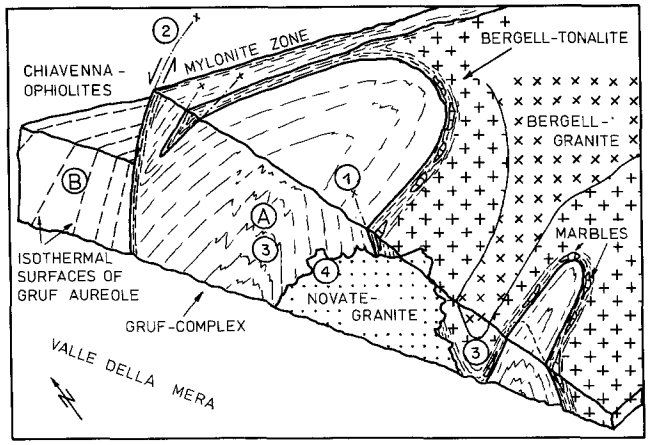

Fig. 17. Schematic geological block diagram of the Gruf-Complex. (A) Block of Gruf and Bergell rocks experienced strong and rapid differential uplift, (B) surrounding Pennine nappe system. Recognizable succession of geological events: 1) emplacement of Bergell rocks above Gruf complex, 2) period of strong differential uplift, formation of contact aureole in (B), 3) folding, 4) intrusion of Novate granite

tures *and* pressures prior to the *PT*-conditions calculated from thermobarometry. Although the maximum conditions reached are unknown and earlier stages are poorly preserved it seems reasonable to assume that *all* metapelites of the Gruf-complex experienced the same metamorphic history, and hence that *all* Gruf metapelites followed the *P-T*-trajectory deduced by Droop and Bucher (1983) for the Bresciadega sapphirine-bearing rocks (Fig. 16). The maximum conditions of 10 kb and 810° C may thus also apply to the rocks examined in this paper. The assemblages orthopyroxene + quartz and orthopyroxene + K-feldspar found in magnesian metapelites are strong evidence for this.

A pressure of 3.5 to 4 kb was estimated for the Chiavenna ophiolites north of the Gruf-complex by Schmutz (1976). Heitzmann (1975) published a pressure estimate of about 5 kb for the area west of the Gruf-complex and a pressure estimate of 3 kb was given by Trommsdorff and Evans (1977) for the area east of the Gruf-complex. The pressure of about 4 kb calculated for the last equilibration of the Gruf rocks coincides with the regional pressure regime of the area. However, as suggested above, if the Gruf-complex was at significantly higher pressures before the last equilibration event it must have experienced a strong differential uplift relative to the surrounding penninic nappe system. Such a marked differential uplift has been documented for the Bergell-Gruf area by Wagner et al. (1979) from a systematic study of apatite fission tracks. They also concluded that differential uplift was very fast in geological terms. It seems therefore, that the Gruf-complex after reaching its maximum prograde *PT*-conditions at about 10 kb and 810° C, experienced a dramatic period of rapid uplift, which ceased in the vicinity of 4 kb. From this point it shared the further metamorphic history with the surrounding units. However, due to the *rapid* uplift the Gruf rock mass must have stored considerable heat. This is confirmed by the contact aureole produced by the Gruf-complex in the Chiavenna ophiolites. A very closely spaced series of isograds in ultramafic rocks ranging from antigorite + forsterite schists to enstatite + forsterite felses were reported from the Chiavenna ophiolites by Schmutz (1976). All samples we collected from ultramafic rocks from the Gruf-complex contained the characteristic assemblage orthopyroxene + forsterite + tremolite + green spinel + chlorite. This assemblage requires temperatures near 800° C at 9–10 kb for $P_{(H_2O)} = P_{(tot)}$ (Evans 1977) in agreement with the temperatures deduced from the sapphirine rocks. The isograds in the Chiavenna ophiolites run parallel to the northern contact of the Gruf-complex. In addition, along the northern contact recrystalized mylonite zones have been mapped and described by Schmutz (1976) and Wenk and Cornelius (1977). The mineralogical compositions of the mylonites are identical to those of other rocks of the Gruf-complex. Liddell et al. (1976) concluded from the study of mylonized quartzites of the Gruf-complex that mylonite formation was a synmetamorphic event. The formation of the mylonites is therefore most likely related to the uplift of the Gruf area from 10 up to 4 kb. The geological relations imply that the uplift was greatest in the north and decreased towards the south.

The relations to the Bergell intrusive complex are controversal. The contact between Bergell intrusive rocks and the Gruf unit seems to be of tectonic nature and both units shared a significant portion of their younger (Alpine) geological history. This is particularly the case for the rapid uplift event. No contact aureole was produced either by the hot Bergell rocks in the Gruf unit or by the Gruf rocks in the Bergell complex. No marked temperature contrasts apparently ever existed between the two units.

A summary of the geological conclusions are sketched on a schematic block diagram (Fig. 17) for the area east of Valle della Mera. The recognizable geological events are numbered from oldest (1) to youngest (4). These are for the Gruf-complex (A): 1) Emplacement of Bergell intrusives on top of the Gruf unit, 2) rapid differential uplift along the northern mylonite contact zone, reequilibration of the Gruf rocks at 3–4 kb and 600–650 deg., formation of the

contact aureole in the Chiavenna ophiolites (B). Differential uplift ceases and the Gruf-Bergell unit shares the metamorphic history with the surrounding penninic nappes, 3) folding (open folds with steep axial planes) related to formation of the steep zone along the Insubric line, 4) intrusion of the Novate granite.

Appendix

The coordinates of equilibrium conditions of mineral reactions in the pressure versus temperature diagrams presented in this paper were obtained as follows:

The thermodynamic properties for all solid phases at 298 K and 1 b were taken from Helgeson et al. (1978) except for Mg-cordierite, phlogopite, spinel and pyrope. For the later phases the data derived by Bucher-Nurminen and Baumgartner (in prep) were employed. The data are given on Table 2 and are consistent with the data base of Helgeson et al. (1978). Thermodynamic properties of phases and reactions at a given P and T were calculated from equations given in Helgeson et al. (1978). The following activity-composition relations have been used in order to calculate the free energy contribution of mixing expressed by the equation:

i) $\Delta G_{P,T} - \Delta G^0_{P,T} = R\,T \ln a$

Where $\Delta G_{P,T}$ denotes the free energy of a given component in solution at P and T, $\Delta G^0_{P,T}$ stands for the free energy of the pure component at P and T, and 'a' represents the activity of the component in the solution. Standard state for all phases is unit activity of the pure phase at any P and T.

1) activity of $KMg_3(AlSi_3)O_{10}(OH)_2$ (phl) in biotite:

$a_{phl} = X^3_{Mg}$

2) activity of $Mg_3Al_2Si_3O_{12}$ (py) in garnet:

$a_{py} = X^3_{Mg}$

3) activity of $Mg_2Al_3(Si_5Al)O_{18}$ (cord) in cordierite:

$a_{cord} = X^2_{Mg}\,(1\text{-}X^{cord}_{H_2O})$

4) activity of $MgAl_2O_4$ (sp) in spinel:

$a_{sp} = X_{Mg}$

5) activity of $MgSiO_3$ (en) in orthopyroxene:

$a_{en} = X_{Mg}$

6) activity of $Mg_7Si_8O_{22}(OH)_2$ (ant) in orthoamphibole:

$a_{ant} = X^7_{Mg}$

7) activity of H_2O in the fluid phase:

$a_{H_2O} = X_{H_2O}$

These solution models are admittedly extremely simple and consequently the resulting PT-coordinates for the equilibrium conditions of the reactions are estimates. However, more sophisticated solution models (e.g. including additional terms for tschermak substitution in orthoamphibole, or provisions for nonideality of enstatite solution in orthopyroxene) do not significantly shift the PT-coordinates for a given reaction. It was found that the maximum temperature difference for a dehydration reaction resulting from the use of the simple models above and more complex ones are typically less than 20° C at a given pressure (tested by using reaction 14) and 15) as examples). Considering all uncertainties involved in the calculations (analytical errors of microprobe analyses, compositional variation of a mineral within one sample, uncertainties in the thermodynamic data), the simple models listed above are unlikely to reduce precision and accuracy significantly.

The mole fractions of H_2O in H_2O-saturated cordierite were calculated from a polynomial expansion in P and T fitted to the experimental data of Mirwald et al. (1979).

The fugacity of pure H_2O at P and T was calculated from the modified Redlich Kwong equation of state published by Jacobs and Kerrick (1981).

Table 2. Thermodynamic properties of minerals

Thermodynamic properties of all phases were taken from Helgeson et al. (1978) except for those listed below. G^0 = free energy of formation from the elements at 298 K and 1 bar (cal/mol), S^0 = third law entropy at 298 K and 1 bar (cal/mol·deg), V^0 = volume at 298 K and 1 bar (ccm/mol). The temperature dependence of the isobaric heat capacity at 1 bar is expressed by the equation:

$cp = a + b\,T - c\,T^{-2}$, a (cal/mol·deg), b (cal/mol·deg^2), c (cal.deg/mol)

1) Phlogopite $KMg_3AlSi_3O_{10}(OH)_2$			
$G^0 = -1392820$	$S^0 = 82.37$		$V^0 = 149.66$
$a = 100.61$	b $= 0.02878$		c $= 2150000$
2) Cordierite $Mg_2Al_4Si_5O_{18}$			
$G^0 = -2063695$	$S^0 = 97.33$		$V^0 = 233.282$
$a = 143.83$	b $= 0.0258$		c $= 3860000$
3) Spinel $MgAl_2O_4$			
$G^0 = -520093$	$S^0 = 19.27$		$V^0 = 39.71$
a $= 36.773$	b $= 0.006416$		c $= 970879$
4) Pyrope $Mg_3Al_2Si_3O_{12}$			
$G^0 = -1417799$	$S^0 = 63.64$		$V^0 = 113.13$
a $= 106.348$	b $= 0.011328$		c $= 2879200$

Acknowledgments. We like to thank Simon Löw for carrying heavy samples out of Val Codera, Kari Vogler for providing unpublished data of his diploma thesis. We also appreciate the stimulating discussions we had with Eduard Wenk and like to thank him for providing the sample Cod6a from the second sapphirine granulite locality, which he recently discovered together with Hans-Ruedi Wenk. We also appreciate the private family fonds made available by Aira Bucher and Barbara Droop to support our field work. We thank F. Seifert for his positive review.

References

Ackermand D, Seifert F (1969) Druck- und Temperaturbedingungen bei der Bildung der sapphirin-führenden Gesteine von Val Codera. Fortschr Mineral 47, Suppl 1, 1

Aranovich LY, Podelesskiy KK (1980) The garnet-plagioclase barometer. Doklady Earth Sci Sec 251:101–103

Barker F (1964) Sapphirine-bearing rock, Val Codera, Italy. Am Mineral 49:146–152

Bethune P de, Laduron D, Bocquet J (1975) Diffusion processes in resorbed garnets. Contrib Mineral Petrol 50:197–204

Bucher-Nurminen K, Baumgartner L (1983) Internally consistent thermodynamic data for phlogopite, Mg-clinochlore, Mg-cordierite, spinel and pyrope. (in prep)

Buehl H (1981) Zur Sillimanitbildung in den Gneisen der Zone von Bellinzona. Schweiz Mineral Petrogr Mitt 61:275–295

Burnham CW, Holloway JR, Davis NF (1969) Thermodynamic properties of water to 1,000° C and 10,000 bars. Geol Soc Am Spec Pap 132, p 96

Cornelius HP (1916) Ein alpines Vorkommen von Sapphirin. Zentralbl Mineral 11:265–269

Cornelius HP, Dittler E (1929) Zur Kenntnis des Sapphirinvorkommens von Alpe Bresciadega in Val Codera (Italien, Prov Sondrio). N Jahrb Mineral 59:27–64

Droop G, Bucher-Nurminen K (1983) Reaction textures and metamorphic evolution of sapphirine-bearing granulites from the Gruf-Complex, Italian Central Alps. J Petrol (in press)

Evans BW (1977) Metamorphism of alpine peridotite and serpentine. Ann Rev Earth Planet Sci 5:397–447

Ferry JM, Spear FS (1978) Experimental calibration of the parti-

tioning of Fe and Mg between garnet and biotite. Contrib Mineral Petrol 66:113–117
Frey M, Hunziker JC, Frank W, Bocquet J, Dal Piaz GV, Jäger E, Niggli E (1974) Alpine metamorphism of the Alps – A review. Schweiz Min Petr Mitt 54:247–290
Ghent ED, Robbins DB, David B, Stout MZ (1979) Geothermometry, geobarometry, and fluid compositions of metamorphosed calcsilicates and pelites, Mica Creek, British Columbia. Am Mineral 64:874–885
Grant JA (1981) Orthoamphibole and orthopyroxene relations in high-grade metamorphism of pelitic rocks. Am J Sci 281:1127–1143
Grant JA, Weiblen PW (1971) Retrograde zoning in garnet near the second sillimanite isograd. Am J Sci 266:908–931
Gulson BL (1973) Age relations in the Bergell region of the South-East Swiss Alps: With some geochemical comparisons. Eclogae Geol Helv 66:293–313
Harley SL, Green DH (1982) Garnet-orthopyroxene barometry for granulites and peridotites. Nature 300:697–701
Heitzmann P (1975) Zur Metamorphose und Tektonik im südöstlichen Teil der Lepontinischen Alpen (Provincia di Como, Italia). Schweiz Mineral Petrogr Mitt 55:467–522
Helgeson HC, Delany JM, Nesbitt HW, Bird DK (1978) Summary and critique of the thermodynamic properties of rock-forming minerals. Am J Sci 278-A
Holdaway MJ, Lee SM (1977) Fe-Mg cordierite stability in high grade pelitic rocks based on experimental, theoretical, and natural observations. Contrib Mineral Petrol 63:175–198
Jacobs GK, Kerrick GK (1981) APL and FORTRAN programs for a new equation of state for H_2O, CO_2 and their mixtures at supercritical conditions. Comp Geosci 7:131–143
Liddell NA, Phakey PP, Wenk HR (1976) The microstructure of some naturally deformed quartzites. In: Wenk HR (ed) Electron microscopy in mineralogy, Springer, Berlin Heidelberg New York, pp 419–427
Milnes AG, Pfiffner AO (1980) Tectonic evolution of the Central Alps in the cross section St. Gallen-Como. Eclogae Geol Helv 73, 619–633
Mirwald PW, Marsch MV, Schreyer W (1979) Der Wassergehalt von Mg-Cordierit zwischen 500° und 800° C sowie 0.5 und 11 Kbar. Fortschr Mineral 57, Beih 1:101–102
Misch P, Rice JM (1975) Miscibility of tremolite and hornblende in progressive Skagit metamorphic suite, North Cascades, Washington. J Petrol 16:1–21
Moticska P (1970) Petrographie und Strukturanalyse des westlichen Bergeller Massivs und seines Rahmens. Schweiz Mineral Petrogr Mitt 50:355–444
Newton RC, Haselton HT (1981) Thermodynamics of the garnet-plagioclase-Al_2SiO_5-quartz geobarometer. In: Thermodynamics of minerals and melts (eds) Newton, Navrotsky, Wood, Springer, Berlin Heidelberg New York
Newton RC, Wood BJ (1979) Thermodynamics of water in cordierite and some petrologic consequences of cordierite as a hydrous phase. Contrib Mineral Petrol 68:391–405
Schmid R, Wood BJ (1976) Phase relationships in granulitic metapelites from the Ivrea-Verbano zone (Northern Italy). Contrib Mineral Petrol 54:255–279
Schmutz HU (1976) Der Mafitit-Ultramafitit-Komplex zwischen Chiavenna and Val Bondasca. Beitr Geol Karte Schweiz NF 149, p 73
Stormer JC, Whitney JA (1977) Two-feldspar geothermometry in granulite facies metamorphic rocks. Sapphirine granulites from Brazil. Contrib Mineral Petrol 65:123–133
Thompson AB (1976) Mineral reactions in pelitic rocks. II. Calculation of some $P-T-X$(Fe−Mg) phase relations. Am J Sci 276:425–454
Thompson JB (1982) Composition space: An algebraic and geometric approach. In: Ferry JM (ed) Characterization of metamorphism through mineral equilibria. Rev Mineral 10:1–31
Trommsdorff V (1980) Alpine metamorphism and Alpine intrusions. In: Geology of Switzerland, a guide book, Part A: An outline of the Geology of Switzerland. Schweiz Geol Kommission (ed), Wepf, Basel, pp 82–87
Trommsdorff V, Evans BW (1977) Antigorite-Ophicarbonates: Contact Metamorphism in Valmalenco, Italy. Contrib Mineral Petrol 62:301–312
Vogler K (1983) Petrographie und Mineralogie von Pegmatiten und ihren Nebengesteinen im Gebiete des Pizzo Trubinasca (Oberes Val Codera). Diplomarbeit, Univ Basel, p 92
Wagner GA, Miller DS, Jäger E (1979) Fission track ages on apatite of Bergell rocks from Central Alps and Bergell boulders in oligocene sediments. Earth Planet Sci Lett 45:355–360
Wells PDA, Richardson SW (1980) In Caledonides of the British Isles – reviewed. Harris AL, Holland CH, Leake BE (eds) Geol Soc London Spec Publ 8:339–344
Wenk E, Keller F (1969) Isograde in Amphibolitserien der Zentralalpen. Schweiz Mineral Petrogr Mitt 49:157–198
Wenk HR (1973) The structure of the Bergell Alps. Eclogae Geol Helv 66:255–291
Wenk HR, Wenk E, Wallace JH (1974) Metamorphic mineral assemblages in pelitic rocks of the Bergell Alps. Schweiz Mineral Petrogr Mitt 54:507–554
Wenk HR, Cornelius SB (1977) Geologischer Atlas der Schweiz, 1:25'000, Blatt Sciora. Publ Schweiz Geol Kommission
Wood B (1974) The solubility of alumina in orthopyroxene coexisting with garnet. Contrib Mineral Petrol 46:1–15
Woodsworth G (1977) Homogenization of zoned garnets from pelitic schists. Can Mineral 15:230–242
Wyllie PJ (1977) Crustal anatexis: An experimental review. Tectonophys 43:41–71
Yardley B (1977) An empirical study of diffusion in garnet. Am Mineral 62:793–800

Received July 25, 1983; Accepted August 4, 1983